Eur Biophys J (2004) 33: 98–108
DOI 10.1007/s00249-003-0332-9

ARTICLE

H. Mozsolits · T.-H. Lee · A. H. A. Clayton
W. H. Sawyer · M.-I. Aguilar

The membrane-binding properties of a class A amphipathic peptide

Received: 13 February 2003 / Revised: 12 May 2003 / Accepted: 13 May 2003 / Published online: 18 July 2003

Abstract The membrane-binding properties of a class A amphipathic peptide (18D) were investigated using two different immobilized model membrane systems. The first system involved the use of surface plasmon resonance (SPR) to study the binding of 18D to dimyristylphosphatidylcholine (DMPC) and dimyristylphosphatidylglycerol (DMPG), which allowed peptide binding to be monitored in real time. The SPR experiments indicated stronger binding of 18D to DMPG than DMPC, which kinetic analysis revealed was due to a faster on-rate. The second model membrane system involved immobilized membrane chromatography in which the binding of 18D to either DMPC or DMPG monolayers covalently linked to silica particles was analysed by elution chromatography. Stronger binding affinity of 18D was also obtained with the negatively charged phosphatidylglycerol (PG) monolayer compared to the phosphatidylcholine (PC) monolayer, which was consistent with the SPR results. Non-linear binding behaviour of 18D to the immobilized lipid monolayers was also observed, which suggests that the peptide undergoes conformational and orientational changes upon binding to the immobilized PC and PG ligands. Significant band broadening was also observed on both monolayers, with larger bandwidths obtained on the PC surface, indicating slower binding and orientation kinetics with the zwitterionic surface. The dependence of log*k*' on the percentage of methanol also demonstrated a bimodal interaction whereby hydrophobic forces predominated at higher temperatures and methanol concentrations, while at lower temperatures, electrostatic and other polar forces also made a contribution to the affinity of the peptides for the lipid monolayer particularly. Overall, these results demonstrate the complementary use of these two lipid biosensors which allows the role of hydrophobic and electrostatic forces in peptide–membrane interactions to be studied and insight gained into the kinetic factors associated with these interactions.

Keywords Amphipathic α-helix · Immobilized lipid chromatography · Membrane affinity · Peptide–membrane interaction · Surface plasmon resonance

This paper was submitted as a record of the 2002 Australian Biophysical society

H. Mozsolits · T.-H. Lee · M.-I. Aguilar (✉)
Department of Biochemistry and Molecular Biology,
Monash University, 3800 Clayton,
Vic, Australia
E-mail: mibel.aguilar@med.monash.edu.au
Tel.: +61-3-99053723
Fax: +61-3-99055882

A. H. A. Clayton · W. H. Sawyer
The Russell Grimwade School of Biochemistry
and Molecular Biology,
The University of Melbourne,
Parkville, Australia

Introduction

Lipoproteins are soluble aggregates of lipids and proteins that efficiently transport hydrophobic, water-insoluble triglyceride and cholesteryl esters from the liver and intestine to other tissues in the body via the bloodstream. The stable non-covalent assemblies of lipoprotein particles are spherical in shape and consist of a neutral lipid core (triglyceride and cholesteryl ester) surrounded by a surface monolayer of phospholipids, unesterified cholesterol and proteins. Apolipoproteins are the major protein components found in lipoproteins, which have been broadly classified into two groups, exchangeable apolipoproteins (A-I, A-II, A-IV, C-I, C-II, C-III and E) and non-exchangeable apolipoproteins (B-100 and B-48) (Segrest et al. 1992). Structural analysis has revealed that the amphipathic helix is a common structural motif in apolipoproteins (Segrest et al. 1974, 1992). In particular, these amphipathic helices have important roles in modulating the lipid-binding properties of apolipoproteins and in determining the size and stabilizing the structure of the lipoprotein particles (Epand et al. 1995).

The helical segments in the exchangeable apolipoproteins have been classified as class A amphipathic helices, based on amino acid sequence analysis of lipid-associating domains of apolipoproteins using helical wheel projections (Segrest et al. 1990). The class A amphipathic helices are characterized by a specific distribution of charged residues in which the positively charged residues are found at the polar–non-polar interface and negatively charged residues are located at the centre of the polar face. The positively charged residues have an important role in interacting with the negatively charged membrane surface of the cell membrane and lipoprotein particles (Lund-Katz et al. 1995) and the class A helices in apolipoproteins are also critical in stabilizing the membrane and preventing leakage of cellular contents by reducing the negative curvature strain of the membrane (Epand et al. 1995; Tytler et al. 1993).

The affinity of these helices for lipids is thus an important parameter to determine and is controlled by various properties, such as the distribution of polar, charged residues in the polar face, the hydrophobicities of non-polar residues in the non-polar face, the magnitude of the hydrophobic moment and the degree of helicity. The conformation of a range of peptide analogues in aqueous solution, trifluoroethanol (TFE) and bound to lipid membranes have been characterized by various techniques, such as circular dichroism and attenuated total reflection FTIR (Clayton and Sawyer 1999; Corijn et al. 1993; Mishra and Palgunachari 1996). A conformational transition from an extended structure to a helical structure has been shown to occur for these peptides after binding to lipid vesicles. The affinity and binding kinetics with various phospholipids of class A amphipathic peptides have also been studied by centrifugation and fluorescence quenching and have shown an increased binding affinity and faster kinetics of class A peptides binding to vesicles containing negatively charged phospholipids compared to zwitterionic phosphatidylcholine vesicles (Polozov et al. 1998). The orientation of these helices relative to the membrane surface has also been studied by fluorescence techniques with a series of peptide analogues (Clayton and Sawyer 1999) containing a tryptophan residue at different positions along the peptide sequence. The results of acrylamide quenching of tryptophan residues and second-derivative absorption spectrum analysis of a tyrosine residue indicated that these peptides align predominantly parallel to the unilamellar egg phosphatidylcholine membrane surface, with the polar face directed towards the aqueous phase and the non-polar face embedded in the membrane interfacial region.

In the present study we have used two complementary lipid biosensors to directly analyse the membrane-binding behaviour of a class A helix. In previous studies we have demonstrated the use of surface plasmon resonance techniques to quantitate the binding affinity of peptides for different membrane surfaces (Lee et al. 2001; Mozsolits and Aguilar 2002; Mozsolits et al. 2001, 2002; Subasinghe et al. 2003). In addition, we have also synthesized and characterized a series of immobilized phospholipid monolayers which were shown to be a stable and sensitive system for the analysis of peptide–membrane interactions (Lee et al. 2001; Mozsolits et al. 1999). In order to analyse the binding of such class A amphipathic peptides to lipid membranes, the binding of one such class A peptide, 18D, which is known to adopt helical structure and bind parallel to the membrane surfaces, was investigated using the two complementary immobilized lipid biosensors.

Materials and methods

Peptide synthesis and purification

The 18D peptide, DRLKAFYDKVAWKLKEAF, was prepared by solid-phase peptide synthesis using standard Fmoc chemistry on an HMP resin with an automated Applied Biosystems Peptide Synthesizer 441A (Clayton and Sawyer 1999). The crude peptides were purified by semi-preparative RP-HPLC (C18 column) using linear gradient elution from 10% to 70% acetonitrile/Mill-Q/0.1% trifluoroacetic acid in 60 min with a flow rate of 3 mL/min. The purified 18D peptide was analysed by analytical RP-HPLC, which showed greater than 99% purity. The amino acid sequence and other physical properties of 18D are listed in Table 1.

Immobilized lipid monolayers

The immobilizable phosphatidylcholine and phosphatidylglycerol were covalently attached to 3-isothiocyanatopropyltriethoxy (ITCPS) modified ZORBAX Rx-SIL silica particles (5 μm diameter and 300 Å average pore size) as previously described (Lee et al. 1999). The silica was dried under reduced pressure for 24 h and stored under anhydrous conditions until use.

Preparation of DMPC vesicles and fluorescence labelling

A small amount of DMPC dissolved in 2 mL of chloroform/methanol (1:1) was placed in a clean, dry test-tube and the solvent evaporated under a stream of dry nitrogen for 2 h. The resulting lipid film was placed under vacuum overnight to ensure complete removal of organic solvent. The multilamellar vesicles (MLV) were prepared at room temperature with the addition of 10 mL Milli-Q water to the dried lipid film. The solution was then vortexed at high speed for 5 min and formed a turbid DMPC-MLV suspension.

Labelling of the DMPC-MLV and the immobilized phospholipid monolayer on the silica particles with the fluorescence probe was achieved by adding 3 μL of 1,6-diphenyl-1,3,5-hexatriene (DPH) (1 mM in tetrahydrofuran) to 3 mL of DMPC-MLV suspension and to 3 mL of lipid-immobilized silica particle suspension (0.3 mg/mL). The suspension was kept at 5°C for 2 h, enabling the partition of DPH molecules into the hydrocarbon core of the lipid

Table 1 Sequence characteristics of 18D and NATA

Peptide	Sequence	MW	μ_H[a]	Charge[b]
18D	DRLKAFYDKVAWKLKEAF	2228	0.81	2+
NATA	Ac-W-NH_2	245	–	–

[a]The hydrophobic moments of 18D were calculated as described by Eisenberg et al. (1982)
[b]Total net charge based on the number of positively and negatively charged amino acids

monolayer/bilayers. Light exposure was avoided at all times for DPH-probed DMPC-MLV and lipid immobilized silica preparations.

Fluorescence measurements

Fluorescence measurements were made with a SPEX Fluorolog Tau 2 spectrometer with a 600 W Xe-Hg lamp as the excitation source. The fluorescence data were recorded using vertically polarized excitation with the emission collected in the right angle geometry. An excitation wavelength of 360 nm was used excite the DPH molecules. The emission wavelength was 426 nm. The emission polarizer was set to 55° relative to the vertical polarization axis of the exciting light to eliminate polarization bias artifacts resulting from the emission monochromator grating and the fluorophore, and to reduce contributions from vesicle and silica particle scattering.

Steady-state anisotropies were measured in the L-format (single channel) with the slit width adjusted to 4 mm. The DPH anisotropies were calculated as $r = (I_{vv} - GI_{vh})/(I_{vv} + 2GI_{vh})$ with a grating correction factor (G factor) to account for differences in monochromator sensitivity to vertically (vv) and horizontally (vh) polarized light. Ten spectral signals were averaged to obtained an adequate signal-to-noise ratio. Samples were placed in a closed, thermostated circulating system and the temperature was monitored from 5 °C to 55 °C.

Chemicals and reagents

N-Octyl-β-D-glucopyranoside, dimyristoyl-L-α-phosphatidylcholine (DMPC), dimyristoyl-L-α-phosphatidyl-DL-glycerol (DMPG), bovine serum albumin (BSA) and *N*-acetyl-L-tryptophanamide (NATA) were purchased from Sigma (St Louis, Mo., USA). Methanol (HPLC) grade was obtained from Mallinckrodt Baker (Paris, Ky., USA).

Surface plasmon resonance studies

Apparatus

Biosensor experiments were carried out with a BIACORE X analytical system (Biacore, Uppsala, Sweden) using the Pioneer L1 sensor chip (Biacore) as previously described (Mozsolits et al. 2001). The L1 sensor chip is composed of alkyl chains covalently linked to a dextran-coated gold surface. The running buffer used for all experiments was phosphate buffer (0.02 M NaH_2PO_4/Na_2HPO_4, pH 6.8). The washing solution was 40 mM CHAPS. The regeneration solution was 10 mM sodium hydroxide. All solutions were freshly prepared, degassed and filtered through a 0.22 μm filter. The operating temperature was 25 °C.

Liposome preparation and formation of supported lipid bilayer

Small unilamellar vesicles of DMPC or DMPG (SUV 50 nm) were prepared in 0.02 M phosphate buffer by sonication, as previously described (Mozsolits et al. 2001). After cleaning as outlined in the instrument manual, the BIACORE X instrument was left running overnight using Milli-Q water as eluent to thoroughly wash all liquid handling parts of the instrument. The L1 sensor chip was then installed and the alkanethiol surface was cleaned by an injection of the non-ionic detergent 40 mM CHAPS (25 μL), at a flow rate of 5 μL/min. SUV (30 μL, 0.5 mM) were then immediately applied to the chip surface at a low flow rate (2 μL/min). To remove any multilamellar structures from the lipid surface, sodium hydroxide (30 μL, 10 mM) was injected at flow rate of 50 μL/min, which resulted in a stable baseline corresponding to the supported lipid bilayer, as previously shown (Mozsolits et al. 2001).

Peptide binding to the bilayer membrane

Peptide solutions were prepared by dissolving 18D in phosphate buffer from 10 to 100 μM. The solutions (80 μL, 980 s) were injected over the lipid surface at a flow rate of 5 μL/min. The peptide solution was then replaced by phosphate buffer and the peptide–membrane complex allowed to dissociate for 1200 s. All binding experiments were carried out at 25 °C. The affinity of 18D for the lipid bilayer membrane was determined from analysis of a series of response curves collected at 10 different peptide concentrations injected over each lipid surface. The peptide concentrations ranged from 10 to 100 μM for both phosphoplipids. Binding curves were also obtained for 18D at 60 μM at flow rates from 2 to 50 μL/min and the data showed that the initial binding rate of the 18D peptide did not vary notably with flow rate, indicating that the peptide–membrane interaction was not mass transport limited.

Numerical integration analysis

The sensorgrams were analysed by curve fitting using numerical integration analysis (Karlsson and Falt 1997; Morton et al. 1995). The BIAevaluation software offers seven different reaction models to perform complete kinetic analyses of the peptide sensorgrams. As previously described, the simple Langmuir binding 1:1 reaction model results in a poor fit when applied to antimicrobial peptide–lipid interactions (Lee et al. 2001; Mozsolits et al. 2001). Two more complex curve-fitting algorithms, namely the two-state and the parallel reaction models, were then chosen for comparison, on the basis of what is known about the possible binding mechanisms of class A peptides. The data were then fitted globally by simultaneously fitting the peptide sensorgrams obtained at 10 different concentrations. The two-state reaction model describes two reaction steps which, in terms of peptide–lipid interaction, may correspond to (1) peptide (P) binding to lipids (L) to give PL followed by (2) the complex PL changing to PL*, which cannot dissociate directly to P + L and which may correspond to partial insertion of the peptide into the hybrid bilayer membrane. The corresponding differential rate equations for this reaction model are represented by:

$$dR_1/dt = k_{a1}C_A(R_{max} - R_1 - R_2) - k_{d1}R_1 - k_{a2}R_1 + k_{d2}R_2 \quad (1)$$

$$dR_2/dt = k_{a2}R_1 - k_{d2}R_2 \quad (2)$$

The parallel reactions model was also applied to each data set. This model assumes that two simple bimolecular interactions occur in parallel with different rate constants, giving a complex bimolecular interaction. To facilitate comparison of the SPR data with the immobilized lipid chromatography data, only the data for the two-state model is reported in the present study. This does not however preclude the possibility that a parallel reactions model or indeed more complex models may contribute to the complex binding mechanism of 18D with the bilayer membrane.

Chromatographic analysis

Column packing

The glycerophospholipid-immobilized silica particles, PC-Si and PG-Si, were packed separately into analytical HPLC columns. The modified porous silica particles (1.5 g) were suspended in 35 mL of vacuum-degassed isopropanol and sonicated for 10 min to ensure even particle dispersion and to remove the air entrapped in the pore system of the particles. The silica suspension was packed into a 4.6 mm i.d.×40 mm custom-made stainless-steel column (SGE, Australia) using a Shandon column packer (Shandon Southern Products, Cheshire, UK). The instantaneous packing pressure was kept constant at 5500 psi. The packing configuration was firstly upward packing with 100 mL of

isopropanol flowing through the column, followed by inversion to the downward configuration during passage for another 40 mL of isopropanol.

Chromatographic and computational procedures

All chromatographic measurements were performed on a Beckman System Gold chromatographic system (Beckman Instruments, Fullerton, Calif., USA) consisting of a dual-pump programmable solvent module 126, variable UV detector module 166, autosampler module 507 and IBM AT computer with System Gold PC software. All chromatographic data were collected at 214 nm. Further peak analysis was performed using System Gold software version 5.0. The column temperature was controlled by total immersion of the column in a MultiTemp thermostatic circulator (LKB-Producter, Bromma, Sweden). Water was quartz-distilled and de-ionized in a Milli-Q system (Millipore, Bedford, Mass., USA). Bulk solvents and mobile phases were filtered through a 0.22 μm nylon membrane filter (Alltech Associates, Australia) using a Millipore solvent filtration apparatus and degassed by sparging with anhydrous helium for 25 min.

Isocratic elution was performed using 0–70% (v/v) methanol in Milli-Q water and at a flow rate of 1 mL/min. Column temperature was maintained at temperatures of 5, 15, 25, 35, 45, 55 °C and varied by less than 0.5 °C. The effects of concentration on the solute retention on the immobilized PC monolayer were carried out using isocratic elution with 5–200 mM sodium phosphate at 15 and 45 °C. The column was equilibrated at each solvent and temperature for 35 min before the injection of samples. Sample solutions were prepared by dissolving the test molecules in Milli-Q water at a concentration of 1 mg/mL and stored at −25 °C until use. The injection sample size was varied between 0.5 and 1.0 μg. All injections were carried out in duplicate, with retention times typically varying by less than 1 s. The column dead time (t_0) was calculated as the breakthrough peak of water blank monitored as an absorbance change at 214 nm. The retention time for all samples were reproducible after 40 and 60 injections at various methanol concentrations, with only small changes in the peak shape and decreases in the bandwidth measured at 13.4% peak height. Such reproducible retention behaviour indicated that the immobilized glycerophospholipid molecules on the porous silica particles were stable under the aqueous/methanol conditions and the range of temperatures used in this work.

Retention on the immobilized lipid monolayers

The retention of a solute in a high-performance liquid chromatography (HPLC) system is governed by the distribution equilibrium established between the stationary phase and the mobile phases and characterized by the equilibrium constant, K_{eq}:

$$K_{eq} = C_s/C_m \quad (3)$$

where C_s and C_m are the concentration of the solute in the stationary phase and the mobile phase, respectively.

The retention of a solute in the immobilized lipid chromatographic system with isocratic elution is characterized by the capacity factor, k', according to the following expression:

$$k' = (t_r - t_0)/t_0 \quad (4)$$

where t_r is the retention time of the solute and t_0 is the void time of the column. Under conditions where the hydrophobic interactions are the dominant interactive force between the solutes and *n*-alkyl ligands, a linear dependency of solute retention, $\log k'$, on the solvent mole fraction, ϕ, required to elute the solute from the hydrophobic surface can be obtained according to:

$$\log k' = \log k_0 - S\phi \quad (5)$$

where the $\log k_0$ value is the extrapolated $\log k'$ in the absence of organic solvent ($\phi = 0$) and S is the slope of the plot of $\log k'$ versus ϕ over a defined k' range. As shown in various studies (Lee et al. 1999; Mozsolits et al. 1999, 2002), the variation in the binding properties of peptides as a consequence of conformational effects are reflected by the changes in $\log k'$, which provides a sensitive parameter to probe the conformational status of peptides during the interaction with the immobilized lipids.

Results

Surface plasmon resonance experiments

The sequence and the amphipathic nature of the 18D peptide is illustrated as a helical wheel in Fig. 1 and the sequence, molecular weight and hydrophobic moment of 18D are listed in Table 1. The design of 18D was based on the sequence of the peptide 18A derived from apolipoprotein A-I (Venkatachalapathi et al. 1993). 18A is known for its function in the activation of lecithin:cholesterol acyl transferase and competes with the binding of apolipoprotein A-I to phospholipid surfaces (Venkatachalapathi et al. 1993). This peptide contains a tyrosine residue at position 7 whose local environment has been characterized using second derivative absorption spectroscopy (Clayton and Sawyer 1999, 2000a, 2000b). In addition, the tryptophan residue at position 12 of 18D is located at the centre of the polar face of the amphipathic helical structure. Although the hydrophobic moment of 18D is lowered by the presence of a tryptophan residue in the polar face, the peptide was found by CD to adopt an α-helical conformation in egg phosphatidylcholine vesicles (Clayton and Sawyer 1999, 2000a). Oriented CD measurements also illustrated that 18A aligns almost parallel to the membrane surface (Clayton and Sawyer 1999, 2000a).

Zwitterionic DMPC or anionic DMPG lipid vesicles were immobilized on the surface of the L1 sensor chip and used to monitor the binding of the 18D model peptide to the phospholipid surfaces. Figure 2a shows the comparative binding sensorgrams of 18D at a concentration of 60 μM to the immobilized zwitterionic DMPC and anionic DMPG phospholipid surfaces and clearly demonstrates the different binding kinetics of

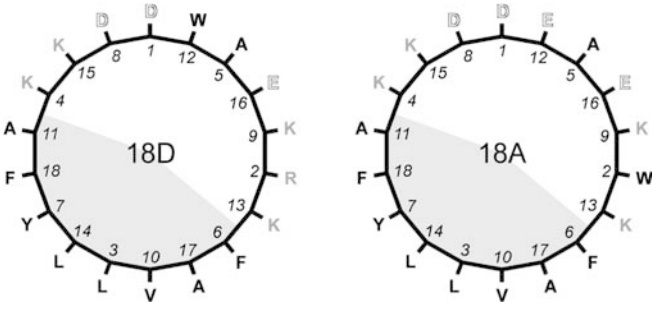

Fig. 1 Schematic representation of the sequence characteristic and amphipathic properties of 18D, which is designed based on peptide 18A (Venkatachalapathi et al. 1993). The non-polar residues are coloured in *black* and the positively charged residues are coloured in *gray*, whereas as the negatively charged residues are coloured in *white*. The non-polar face of the amphipathic peptide is also indicated by *light gray* colour

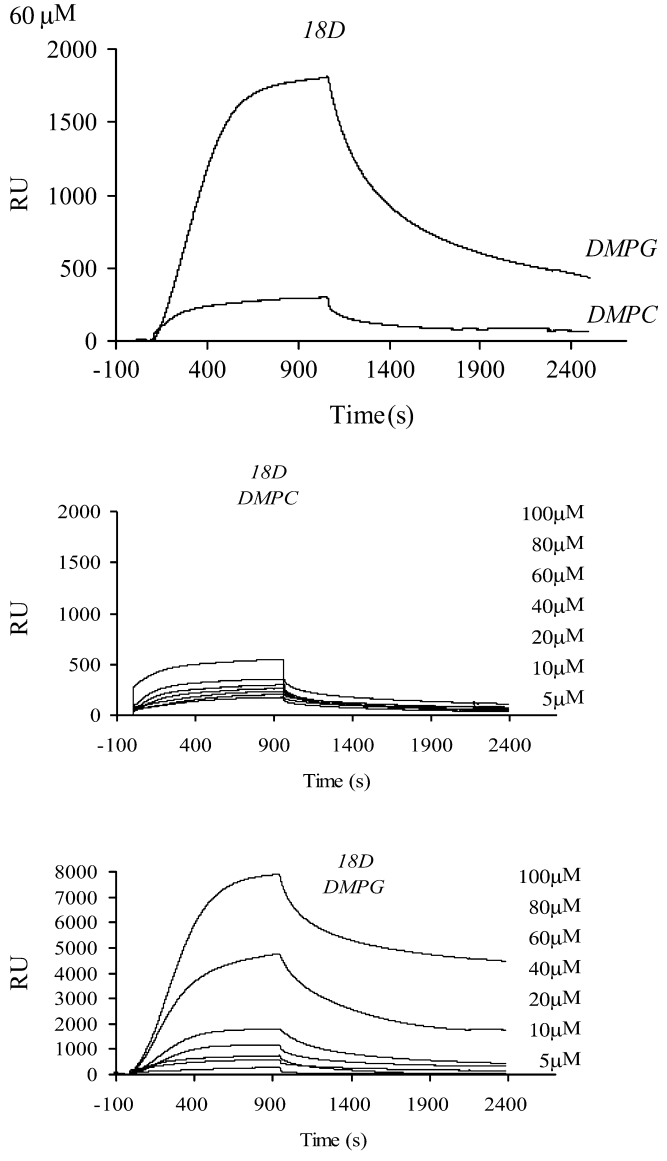

Fig. 2 The binding of 18D (60 μM), a class A amphipathic peptide, to DMPC and DMPG immobilized liposome surfaces. Experimental peptide sensorgrams for the binding of 18D to (**b**) DMPC and (**c**) DMPG liposomes at peptide concentrations of 5–100 μM and (**a**) comparative experimental peptide sensorgrams of 18D

18D to each liposome. Comparison of SPR responses (RU_{max}) indicates that a higher proportion of 18D bound to the negatively charged DMPG than to the zwitterionic DMPC, which suggests a higher affinity for anionic DMPG than the zwitterionic DMPC. As previously observed for a range of amphipathic peptides (Lee et al. 2001; Mozsolits et al. 2001, 2002), an injection of NaOH across the peptide bound surface did not remove 18D from the phospholipid surfaces, indicating a predominantly hydrophobic interaction. However, in contrast to these previous studies, normal buffer flow was able to remove all of the bound 18D from the phospholipid surfaces within a reasonable time, which thus allowed the peptide sensorgrams to return to zero. In these cases, the same immobilized liposome surface could be used for subsequent peptide injections. In the case of anionic DMPG, it took twice as long for the buffer flow to remove all 18D from the phospholipid surface than in the case of zwitterionic DMPC. These results also indicate that 18D neither bound strongly to the phospholipid surfaces nor inserted deeply into the membranes.

Kinetic analysis of the SPR results allowed the association (k_a) and dissociation rate constants (k_d) and the affinity constant (K) for the peptide–membrane interaction to be calculated. For a complete kinetic analysis of the peptide–membrane interactions, multiple sets of peptide sensorgrams using different peptide concentrations (5–100 μM), as shown in Fig. 2b and Fig. 2c, were generated on the immobilized DMPC or DMPG liposome surfaces and numerical integration analysis was applied to the SPR data. As can be seen in Fig. 2c, the correlation between the RU_{max} and the peptide concentrations is not linear at 80 and 100 μM on DMPG. This finding may reflect the aggregation or multilayering of 18D at higher concentrations. The sensorgrams obtained at 80 and 100 μM peptide concentrations were therefore excluded from kinetic analysis on this lipid surface.

As previously observed for other amphipathic peptides (Mozsolits et al. 2001, 2002), the two-state reaction model was selected based on the proposed two-step binding process for membrane-active peptides and provided a superior fit to the data compared to the Langmuir 1:1 model of interaction. The association (k_{a1}, k_{a2}) and dissociation (k_{d1}, k_{d2}) rate constants and the affinity constant (K) estimated by the two-state reaction model are listed in Table 2. The affinity constants listed in Table 2 demonstrate that the binding affinity of the α-helical 18D model peptide for the anionic DMPG is higher compared to that for the zwitterionic DMPC. The initial association rate values in the case of the two-state model indicate that the higher affinity of 18D for DMPG than with DMPC is due to a faster on-rate and slower off-rate. The increased binding affinity is most likely related to the increased electrostatic interaction between the negatively charged head-group region of DMPG and the positively charged residues of 18D, which are located at the polar–non-polar interface of the amphipathic helix, shown in Fig. 1. The overall higher affinity on DMPG also suggests that the electrostatic interactions between the anionic DMPG and the positively charged residues of 18D have further enhanced the hydrophobic binding of 18D to the phospholipids.

Immobilized membrane chromatography

Phase behaviour of the immobilized phospholipid monolayers

We have previously shown that immobilized membrane chromatography can be used to provide insight into

Table 2 Association (k_{a1}, k_{a2}) and dissociation (k_{d1}, k_{d2}) rate constants determined by numerical integration using the two-state reaction model, and the affinity constant (K) determined as $(k_{a1}/k_{d1})\times(k_{a2}/k_{d2})$

Peptide	Lipid type	k_{a1} (M^{-1} s^{-1})	k_{d1} (s^{-1})	k_{a2} (M^{-1} s^{-1})	k_{d2} (s^{-1})	K
18D	DMPC	53	56×10^{-4}	11×10^{-4}	6.5×10^{-4}	1.6×10^{4}
	DMPG	81	31×10^{-4}	4.2×10^{-4}	1.0×10^{-4}	11×10^{4}

the role of hydrophobic and electrostatic interactions in peptide–membrane interactions (Lee et al. 1999; Mozsolits et al. 1999, 2002). In order to further validate the use of the immobilized lipid particles for use as a model membrane surface, the membrane-like properties of the immobilized lipid monolayers were investigated by the influence of temperature on the phase transition of immobilized lipid ligands. The phase behaviour of the immobilized lipid monolayer on the silica support was studied by measuring the gel-to-liquid phase transition temperature (T_m) of the lipids. T_m was determined by the fluorescence anisotropy of the probe 1,6-diphenyl-1,3,5-hexatriene (DPH) inserted into the hydrocarbon core of the lipid monolayer. A typical fluorescence anisotropy versus temperature curve for multilamellar DMPC vesicles is shown in Fig. 3a. The dependence of DPH anisotropy on temperature exhibited a distinctive cooperative main chain (order/disorder) transition from the rippled gel ($P_{\beta'}$) phase to a lamellar liquid crystalline ($L\alpha$) phase with a characteristic $T_m = 23.6$ °C, for the multilamellar DMPC vesicles (Koynova and Caffrey 1998).

The DPH anisotropy values versus temperature for the immobilized PC and PG monolayers are shown in Fig. 3a and Fig. 3b, while the dependence of DPH anisotropy on temperature for unmodified silica particles as a control is also shown in the inset in Fig. 3b. While there was some fluctuation in the DPH anisotropy for the unmodified silica, it was largely independent of temperature. In contrast, the DPH anisotropy values obtained for immobilized lipid monolayers decreased with increases in the temperature from 15 to 50 °C. Such temperature-dependent behaviour indicated a clear but less-cooperative gel-to-liquid phase transitions for the lipid monolayers immobilized on the silica support. However, as shown in Fig. 3b, T_m was found at 33.0 °C and 35.0 °C for the immobilized PC and PG monolayers, respectively. In addition, the phase transition of immobilized lipids exhibited a broader temperature range and the decreases in the magnitude of DPH anisotropy were smaller than those of DMPC-MLV.

The immobilization of the lipids onto the silica surface therefore resulted in a phase transition that was characterized by a broader temperature range and smaller DPH anisotropic changes. These smaller changes in the DPH anisotropy reflect the limited motional freedom of the lipid molecules due to the covalent attachment at one end of the lipid. Despite these characteristics, these results indicate that the immobilized lipids on the silica surface exist as a reasonably well-organized monolayer.

Retention behaviour

The interactive behaviour of 18D was then studied using the immobilized phospholipid monolayers by analysis of the isocratic retention times obtained at methanol concentrations between 20% and 60% at a constant flow rate of 1 mL/min and at temperatures between 5 and 55 °C. The values of log k' for the binding of 18D to the immobilized lipid monolayer were derived from the retention times according to Eq. (4). The column dead

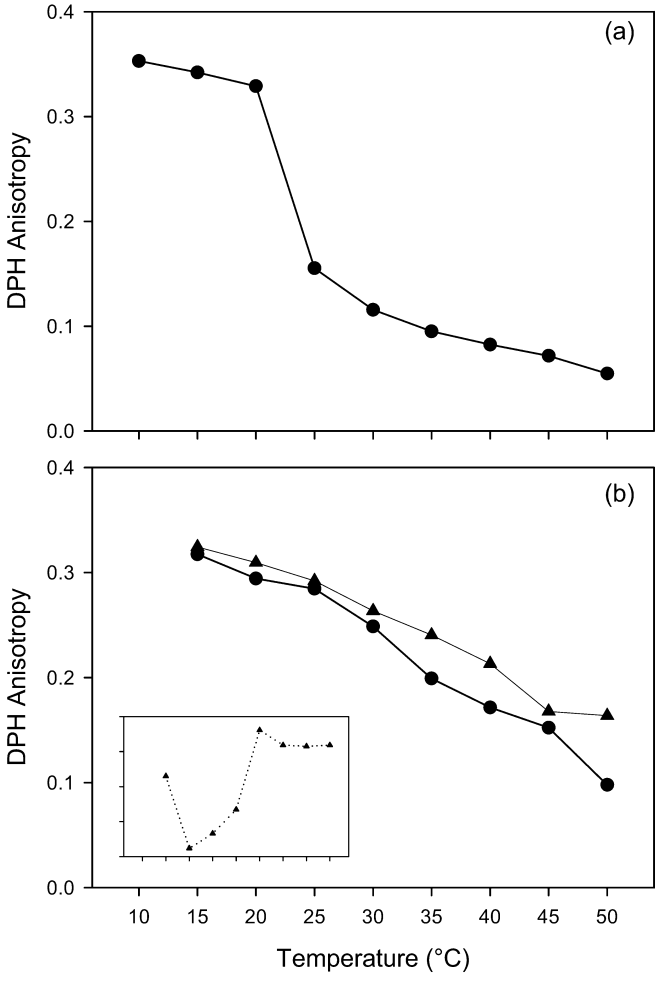

Fig. 3 Temperature-induced changes on DPH anisotropy for (**a**) DMPC multilamellar vesicles and (**b**) immobilized PC (*circles*) and PG (*triangles*) monolayers on silica particles. The *inset* shows the changes in DPH anisotropy for the unmodified silica particles at temperatures between 15 and 50 °C

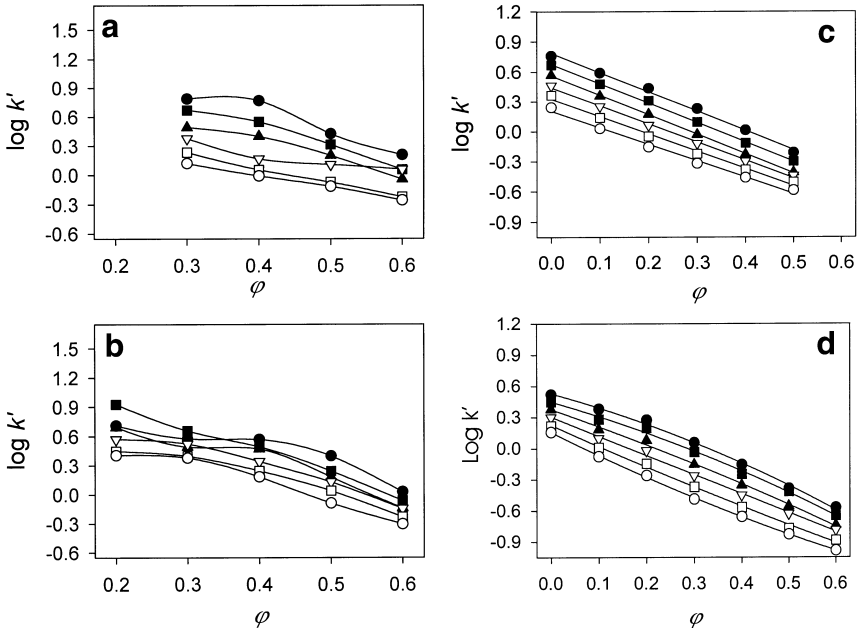

Fig. 4 Dependence of log k' on methanol content for the class A amphipathic peptide, 18D, interacting with the immobilized (**a**) PC and (**b**) PG monolayers and *N*-acetyltrptophanamide interacting with the immobilized (**c**) PC and (**d**) PG monolayers at temperatures of 5 (*filled circles*), 15 (*filled squares*), 25 (*filled up triangles*), 35 (*open down triangles*), 45 (*open squares*) and 55 °C (*open circles*)

time (t_0) was determined from the retention time of the breakthrough peak of a water blank.

The dependences of log k' on the methanol mole fraction (ϕ) for the binding of 18D to the immobilized PC and PG monolayers are shown in Fig. 4a and Fig. 4b, respectively. As shown in Fig. 4a, a general trend of small and relatively linear decreases in log k' with increases in methanol content was observed for 18D binding to the immobilized PC monolayer. However, there were some significant deviations from linearity under some conditions. For example, at 5 °C, log k' values were constant between 30% and 40% methanol, which was then followed by linear decreases in log k' from 40% to 60% methanol. Additionally, at 35 °C, log k' values were relatively independent of methanol concentration between 40% and 60%. The bimodal retention can be compared to the linear behaviour of the small control molecule *N*-acetyl-L-tryptophanamide (NATA) (Fig. 4c), which does not undergo any conformational or insertional changes upon binding (Lee et al. 1999; Mozsolits et al. 1999). Thus the small transition observed at 5 °C and 35 °C for 18D indicates that changes in the structure of the 18D–lipid complex occurred at these temperatures and/or temperature-induced changes in the conformation and motion of lipid molecules which can alter the relative binding affinity of 18D for the immobilized lipid monolayer.

In order to examine the effects of the charge of the phospholipid head group on the binding behaviour of 18D, log k' values for 18D were also obtained on the immobilized PG monolayer. The dependence of log k' values on the methanol content for the binding of 18D to the immobilized PG monolayer (Fig. 4b) showed a similar behaviour to that obtained with the PC monolayer. However, 18D could be eluted with 20% methanol whereas 30% methanol was the minimal methanol concentration required to elute 18D from the PC monolayer. Under most conditions, log k' values were similar to or higher than observed for the PC monolayer. Similar log k' values were obtained at 25–35 °C with the PC and PG monolayers. At 45–55 °C, higher log k' values for 18D were obtained with the PG monolayer than for those with the PC monolayer. These higher log k' values for 18D binding to negatively charged phospholipid monolayers indicates that the positively charged residues located at the polar–non-polar interface of the amphipathic helices increases the binding affinity of 18D to the immobilized PG monolayer. Overall, the retention behaviour of 18D was more complex than the linear dependence of log k' on percent methanol for NATA (Fig. 4d) (Lee et al. 1999; Mozsolits et al. 1999), which does not undergo any conformational/orientational changes during binding. However, 18D had much less complex behaviour than other amphipathic peptides analysed previously (Lee et al. 1999; Mozsolits et al. 1999, 2002), which is consistent with the surface orientation of the peptide (Clayton and Sawyer 1999, 2000a).

Experimental bandwidth properties

The interactive behaviour of 18D with the immobilized lipid monolayers was further assessed through the analysis of elution peak widths. Two major factors can lead to band broadening and peak splitting, namely changes in peptide conformation and changes in the degree of insertion of the peptide into the lipid monolayer. If either of these processes occur with a rate constant that is comparable to the analysis time, band broadening which exceeds that observed for small non-interconverting molecules will be observed (Lee et al. 1999; Mozsolits et al. 1999, 2002). The experimental bandwidth for 18D binding to the immobilized lipid

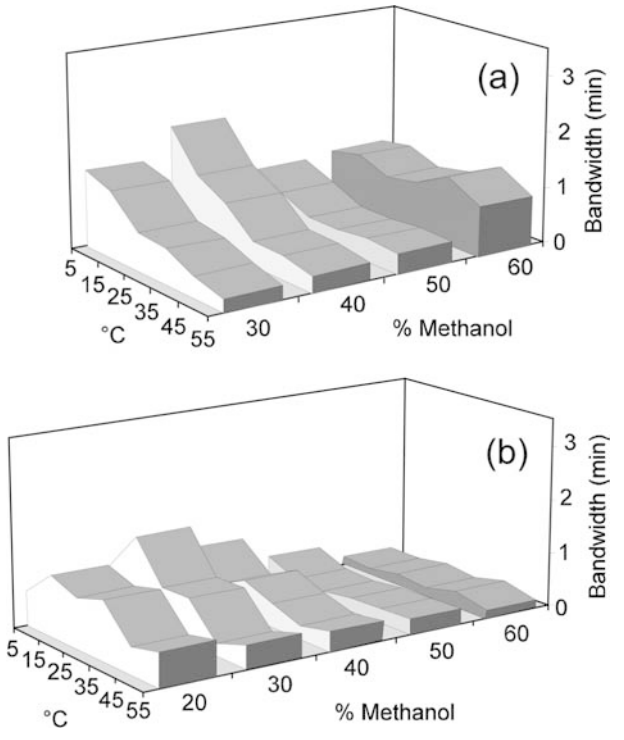

Fig. 5 Bandwidth changes as a function of temperature, 5–55 °C, and methanol concentration for the binding of the class A amphipathic peptide 18D to the immobilized (**a**) PC and (**b**) PG monolayers

monolayers was measured at 4σ (13.4% peak height) and is plotted as a function of temperature and methanol content in Fig. 5. As shown in Fig. 5a, the bandwidth of the elution peaks for the binding of 18D to the immobilized PC monolayer exhibited fluctuations over the range of experimental conditions used. Large increases in the bandwidth were observed at low temperatures between 5 and 15 °C at 30% and 40% methanol. As the temperature increased, a linear decrease in bandwidth was obtained at 30–40% methanol. At 50% methanol, no large increase in bandwidth was observed and the bandwidths were relatively independent of temperature. NATA exhibited no such band broadening, with bandwidths ranging from 0.1 to 0.5 min over the experimental range of temperatures and percent methanol values (Lee et al. 1999; Mozsolits et al. 1999, 2002). Additionally, the bandwidth also increased with increases in temperature. These results indicate that the structural nature of both the peptide and PC ligands changed dramatically at high methanol concentrations and high temperatures.

The dependence of experimental bandwidth on temperature and methanol concentration during the interaction with the immobilized PG monolayer is shown in Fig. 5b, and it is evident that relatively smaller changes in the bandwidth behaviour was observed under most conditions than for PC. Under conditions where conformational and insertional equilibria do not occur, bandwidth values are proportional to log k' values (Mozsolits et al. 1999). However, in the present study, larger log k' values were observed for PG than for PC, while smaller changes in bandwidth were observed with PG than with the PC monolayer. Thus, the conformational and orientational changes which give rise to the non-linear dependence of log k' versus methanol concentration (Fig. 4) are associated with faster rates of interconversions on the PG compared to the PC monolayer.

Discussion

The interaction of peptides with membrane surfaces involves a number of steps which include initial binding to the phospholipids through a mixture of hydrophobic and electrostatic interactions, induction of secondary structure upon binding, reorientation and/or insertion of the peptide into the lipid membrane, and further partitioning of the peptide in the membrane (Shai 1999). The application of surface-sensitive techniques to the study of peptide–membrane interactions represents a powerful approach to the characterization of a wide range of membrane-mediated processes (Heyse et al. 1998). SPR allows the binding of a peptide to a membrane surface to be monitored directly without the need for a specific probe (e.g. fluorescent) or chromophore (as for example in the case of CD and fluorescence spectroscopy). In comparison with other techniques that are used to measure affinity constants, SPR does not rely on the physical separation of bound and free peptide (Wimley and White 1993) and SPR makes no assumption about the secondary structure of the peptide or the degree of insertion into the membrane (Beschiaschvili and Seelig 1990; Niemz and Tirrell 2001; Schwarz and Beschiaschvili 1989; Zhelev et al. 2001). By comparison, immobilized lipid chromatography allows peptide binding to be monitored as a function of both peptide and lipid conformation through changes in temperature and organic solvent concentration. In combination, both techniques can provide information on membrane affinity and the relative contribution of electrostatic and hydrophobic interactions to this interaction. In the present study, we have applied both techniques to the analysis of the membrane-binding properties of a class A amphipathic peptide which has been previously found to bind parallel to the surface of model membranes (Clayton and Sawyer 1999, 2000a).

The SPR experiments demonstrated stronger lipid-binding affinity of 18D for anionic DMPG liposomes than with zwitterionic DMPC liposomes, suggesting a contribution of electrostatic interactions to the binding of 18D to phospholipids. However, since 18D could not be removed from the SPR phospholipid surfaces by an injection of NaOH, which minimizes electrostatic interactions as shown previously for amyloid peptides (Subasinghe et al. 2003), the main interaction between 18D and the phospholipid surfaces at equilibrium is

largely mediated by hydrophobic interactions, as observed previously for other amphipathic peptides (Lee et al. 2001; Mozsolits and Aguilar 2002; Mozsolits et al. 2001, 2002). These results are also confirmed by the non-linear retention plots (Fig. 4) obtained for 18D using immobilized lipid chromatography, which also showed a stronger binding of 18D to the negatively charged lipid monolayer (PG) than the zwitterionic lipid monolayer (PC). Since bound peptide is displaced by increasing methanol concentrations through disruption of hydrophobic interactions, the linear decline in log k' values between 40% and 60% methanol demonstrates a significant contribution of hydrophobic interactions (as compared to the linear plots exhibited by the control molecule *N*-acetyltryptophanamide). By comparison, the constant log k' values observed at lower methanol concentrations indicates that electrostatic and other polar forces also contribute to the binding of 18D.

While methanol does not represent a true physiological solution, in addition to confirming the participation of hydrophobic interactions, the use of increasing amounts of methanol also provides a solution environment in which the conformation of the peptide can be manipulated before binding to the immobilized lipid. At intermediate temperatures which correspond to a transition in either the peptide secondary structure and/or the lipid mobility, complex binding behaviour was observed for 18D. At high temperatures, the peptide will most likely exist as a fully extended coil and will be able to penetrate the lipid chains more extensively than at lower temperatures as a result of the increased lipid mobility. In each case, the binding behaviour is a reflection of the conformational heterogeneity of both the peptide solutes and the immobilized phospholipid.

Comparison of the on-rates obtained by SPR and the bandwidths observed by immobilized lipid chromatography also provides information on the relative rate of binding and conformational changes induced by binding. SPR results indicated a faster on-rate and slower off-rate for the initial binding step with DMPG than for DMPC. In addition, smaller chromatographic bandwidths were observed for PG than for PC, which is also consistent with a faster rate of binding. Moreover, the results of the present study showed smaller changes in the logk' values and bandwidth over the temperature and methanol concentration range for the binding of 18D to the immobilized lipid monolayers than has been previously observed for other amphipathic and antimicrobial peptides (Lee et al. 2001; Lee et al. 1999; Mozsolits et al. 1999). Since 18D has been shown to adopt a helical conformation and orient parallel to the membrane surface, the results suggest that a reduction in insertional equilibrium (or dynamic orientational changes) allowed 18D to dissociate from the SPR surface in a relatively short period of time and also leads to smaller variations in the temperature dependence of log k' and simpler elution profiles, compared to the more complex behaviour observed for hemolytic peptides and peptide hormones (Lee et al. 2001; Lee et al. 1999; Mozsolits et al. 1999, 2002).

The SPR results also correlate with previous studies which examined the binding affinity of other class A amphipathic peptides for phospholipids. For example, Polozov et al. (1998) examined the kinetics and equilibrium membrane binding of class A model amphipathic peptides by centrifugation and fluorescence quenching. The results demonstrated that the class A amphipathic peptides bound stronger to anionic phospholipid vesicles (Ac-18A-NH_2; DOPG; $K = 3.5\times10^6$) than to zwitterionic phospholipid vesicles (Ac-18A-NH_2; DOPC; $K = 4\times10^4$), which was a consequence of faster binding to anionic phospholipid vesicles. In another study, Spuhler et al. (1994) performed thermodynamic analysis of the binding process of two synthesized apolipoprotein A-I model peptides (18A, 18R) to lipid bilayers. It was also found that these model peptides bound more strongly to negatively charged (POPC/POPG) than to zwitterionic POPC membranes. Furthermore, a 40–60% insertion of the model peptides into the hydrophobic membrane region was predicted based on the molecular analysis of the free energy of binding. Gazzara et al. (1997) also investigated the effect of the variation of the amphipathic α-helix structural motif on the lipid-binding properties of five class A amphipathic helical model peptides by fluorescence spectroscopy and titration calorimetry. It was found that two model peptides (18A and Ac-18A-NH_2), that possessed positively charged residues at the interface, bound stronger to phospholipid unilamellar liposomes but the stronger binding was not linked to deeper bilayer penetration. It was concluded that the interaction of class A amphipathic peptides appears to be limited to the membrane surface, with a small level of insertion of the hydrophobic face of the helix into the interior of the bilayer.

Based on the present findings and previous results which showed that 18D adopts an α-helical structure

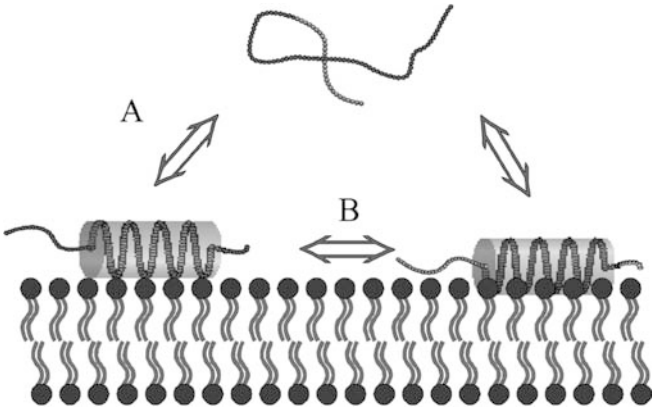

Fig. 6 The binding model of 18D, a class A amphipathic peptide, to membranes. The binding is proposed as a two-step process. **A** The peptide adopts an amphipathic α-helical structure upon contact with lipid and binds electrostatically to localize itself on the surface. **B** Then the peptide relocates and binds hydrophobically to the membrane

upon binding to phospholipids and orients almost parallel to the phospholipid membrane surface (Clayton and Sawyer 1999, 2000a, 2000b), Fig. 6 illustrates a proposed binding model of 18D to phospholipid membranes involving a two-step process. In the first step the peptide, which is unstructured in aqueous solution, adopts an amphipathic α-helical structure and by the aid of electrostatic interactions localizes itself on the membrane surface. In the second step the peptide re-orients itself on the surface and binds via hydrophobic interactions to the membrane surface. Comparison of the two sets of rate constants in Table 2 suggests that step B is considerably slower than step A. Thus the electrostatic interaction between the positively charged residues of the class A amphipathic peptide 18D and the negatively charged lipid head groups enhances the subsequent hydrophobic binding of 18D to the lipid monolayers. A recent study has also demonstrated that a series of class A tryptophan-containing analogues adopts more than one conformation on the lipid surface and the presence of these additional conformational intermediates may also contribute to the multi-step binding mechanism of 18D (Clayton et al. 2003).

In summary, the SPR data has provided, for the first time, experimental data which demonstrate that 18D exhibits a less complex mode of binding in comparison to other amphipathic peptides which insert into the membrane, which is consistent with the surface orientation of 18D. Furthermore, the increased affinity for anionic lipids is not only attributed to a faster on-rate but also a comparatively slower off-rate, again providing new information on the membrane-binding mechanism of this class of peptides. Overall, the combination of two immobilized membrane biosensors further demonstrate the ability of SPR spectroscopy and immobilized lipid chromatography to obtain both equilibrium and kinetic data related to biomolecular interactions, and which in conjunction other spectroscopic techniques can further expand our understanding of the molecular mechanism of peptide–biomembrane interactions mediated by surface adsorption of amphipathic peptides.

References

Beschiaschvili G, Seelig J (1990) Melittin binding to mixed phosphatidylglycerol/phosphatidylcholine membranes. Biochemistry 29:52–58

Clayton AH, Sawyer WH (1999) The structure and orientation of class-A amphipathic peptides on a phospholipid bilayer surface. Eur Biophys J 28:133–141

Clayton AH, Sawyer WH (2000a) Oriented circular dichroism of a class A amphipathic helix in aligned phospholipid multilayers. Biochim Biophys Acta 1467:124–130

Clayton AH, Sawyer WH (2000b) Site-specific tryptophan dynamics in class A amphipathic helical peptides at a phospholipid bilayer interface. Biophys J 79:1066–1073

Clayton AH, Vultureanu AG, Sawyer WH (2003) Unfolding of class-A amphipathic peptides on a lipid surface. Biochemistry 42:(in press)

Corijn J, Deleys R, Labeur C, Vanloo B, Lins L, Brasseur R, Baert J, Ruysschaert JM, Rosseneu M (1993) Synthetic model peptides for apolipoproteins. II. Characterization of the discoidal complexes generated between phospholipids and synthetic model peptides for apolipoproteins. Biochim Biophys Acta 1170:8–16

Eisenberg D, Weiss RM, Terwilliger TC (1982) The helical hydrophobic moment: a measure of the amphiphilicity of a helix. Nature 299:371–374

Epand RM, Shai Y, Segrest JP, Anantharamaiah GM (1995) Mechanisms for the modulation of membrane bilayer properties by amphipathic helical peptides. Biopolymers 37:319–338

Gazzara JA, Phillips MC, Lund-Katz S, Palgunachari MN, Segrest JP, Anantharamaiah GM, Snow JW (1997) Interaction of class A amphipathic helical peptides with phospholipid unilamellar vesicles. J Lipid Res 38:2134–2146

Heyse S, Stora T, Schmid E, Lakey JH, Vogel H (1998) Emerging techniques for investigating molecular interactions at lipid membranes. Biochim Biophys Acta 1376:319–338

Karlsson R, Falt A (1997) Experimental design for kinetic analysis of protein-protein interactions with surface plasmon resonance biosensors. J Immunol Methods 200:121–133

Koynova R, Caffrey M (1998) Phases and phase transitions of the phosphatidylcholines. Biochim Biophys Acta 1376:91–145

Lee TH, Mozsolits H, Aguilar MI (2001) Measurement of the affinity of melittin for zwitterionic and anionic membranes using immobilized lipid biosensors. J Pept Res 58:464–476

Lee T-Z, Rivett D, Werkmeister J, Hewish D, Aguilar MI (1999) The interaction of amphipathic peptides with an immobilised model membrane. Lett Pept Sci 6:371–380

Lund-Katz S, Phillips MC, Mishra VK, Segrest JP, Anantharamaiah GM (1995) Microenvironments of basic amino acids in amphipathic alpha-helices bound to phospholipid: 13C NMR studies using selectively labeled peptides. Biochemistry 34:9219–9226

Mishra VK, Palgunachari MN (1996) Interaction of model class A1, class A2, and class Y amphipathic helical peptides with membranes. Biochemistry 35:11210–11220

Morton TA, Myszka DG, Chaiken IM (1995) Interpreting complex binding kinetics from optical biosensors: a comparison of analysis by linearization, the integrated rate equation, and numerical integration. Anal Biochem 227:176–185

Mozsolits H, Aguilar MI (2002) Surface plasmon resonance spectroscopy: an emerging tool for the study of peptide-membrane interactions. Biopolymers 66:3–18

Mozsolits H, Lee TH, Wirth HJ, Perlmutter P, Aguilar MI (1999) The interaction of bioactive peptides with an immobilized phosphatidylcholine monolayer. Biophys J 77:1428–1444

Mozsolits H, Wirth HJ, Werkmeister J, Aguilar MI (2001) Analysis of antimicrobial peptide interactions with hybrid bilayer membrane systems using surface plasmon resonance. Biochim Biophys Acta 1512:64–76

Mozsolits H, Unabia S, Ahmad A, Morton CJ, Thomas WG, Aguilar MI (2002) Electrostatic and hydrophobic forces tether the proximal region of the angiotensin II receptor (AT1A) carboxyl terminus to anionic lipids. Biochemistry 41:7830–7840

Niemz A, Tirrell DA (2001) Self-association and membrane-binding behavior of melittins containing trifluoroleucine. J Am Chem Soc 123:7407–7413

Polozov IV, Polozova AI, Mishra VK, Anantharamaiah GM, Segrest JP, Epand RM (1998) Studies of kinetics and equilibrium membrane binding of class A and class L model amphipathic peptides. Biochim Biophys Acta 1368:343–354

Schwarz G, Beschiaschvili G (1989) Thermodynamic and kinetic studies on the association of melittin with a phospholipid bilayer. Biochim Biophys Acta 979:82–90

Segrest JP, Jackson RL, Morrisett JD, Gotto AM Jr (1974) A molecular theory of lipid-protein interactions in the plasma lipoproteins. FEBS Lett 38:247–258

Segrest JP, De Loof H, Dohlman JG, Brouillette CG, Anantharamaiah GM (1990) Amphipathic helix motif: classes and properties. Proteins 8:103–117

Segrest JP, Jones MK, De Loof H, Brouillette CG, Venkatachalapathi YV, Anantharamaiah GM (1992) The amphipathic helix in the exchangeable apolipoproteins: a review of secondary structure and function. J Lipid Res 33:141–166

Shai Y (1999) Mechanism of the binding, insertion and destabilization of phospholipid bilayer membranes by alpha-helical antimicrobial and cell non-selective membrane-lytic peptides. Biochim Biophys Acta 1462:55–70

Spuhler P, Anantharamaiah GM, Segrest JP, Seelig J (1994) Binding of apolipoprotein A-I model peptides to lipid bilayers. Measurement of binding isotherms and peptide-lipid headgroup interactions. J Biol Chem 269:23904–23910

Subasinghe S, Unabia S, Barrow CJ, Mok SS, Aguilar MI, Small DH (2003) Cholesterol is necessary both for the toxic effect of Abeta peptides on vascular smooth muscle cells and for Abeta binding to vascular smooth muscle cell membranes. J Neurochem 84:471–479

Tytler EM, Segrest JP, Epand RM, Nie SQ, Epand RF, Mishra VK, Venkatachalapathi YV, Anantharamaiah GM (1993) Reciprocal effects of apolipoprotein and lytic peptide analogs on membranes. Cross-sectional molecular shapes of amphipathic alpha helixes control membrane stability. J Biol Chem 268:22112–22118

Venkatachalapathi YV, Phillips MC, Epand RM, Epand RF, Tytler EM, Segrest JP, Anantharamaiah GM (1993) Effect of end group blockage on the properties of a class A amphipathic helical peptide. Proteins 15:349–359

Wimley WC, White SH (1993) Quantitation of electrostatic and hydrophobic membrane interactions by equilibrium dialysis and reverse-phase HPLC. Anal Biochem 213:213–217

Zhelev DV, Stoicheva N, Scherrer P, Needham D (2001) Interaction of synthetic ha2 influenza fusion peptide analog with model membranes. Biophys J 81:285–304